

A Multi-Mode Dead Reckoning System for Pedestrian Tracking Using Smartphones

Qinglin Tian, *Student Member, IEEE*, Zoran Salcic, *Senior Member, IEEE*,
 Kevin I-Kai Wang, *Member, IEEE*, and Yun Pan, *Member, IEEE*

Abstract—This paper proposes an approach for pedestrian tracking using dead reckoning enhanced with a mode detection using a standard smartphone. The mode represents a specific state of carrying device, and it is automatically detected while a person is walking. This paper presents a new approach, which extends and enhances previous methods by identifying in real-time three typical modes of carrying the device and using the identified mode to enhance tracking accuracy. The way of carrying the device in all modes is unconstrained to offer reliable person-independent tracking. Based on the identification of modes, a lightweight step-based tracking algorithm is developed with a novel step length estimation model. The tracking system is implemented on a commercial off-the-shelf smartphone equipped with a built-in inertial measurement unit with 3-D accelerometer and gyroscope. It achieves real-time tracking and localization performance with an average position accuracy of 98.91%.

Index Terms—Pedestrian dead reckoning, smartphone, real-time tracking, light-weight positioning algorithm, mode-awareness.

I. INTRODUCTION

LOCATION Based Services (LBS) are becoming common in everyday life nowadays. Knowing one's location is helpful in applications such as navigation, Augmented Reality (AR) and assistive healthcare. Global Positioning System (GPS) is able to provide users with sufficiently accurate outdoor locations while performance deteriorates significantly in indoor environment due to signal attenuation within the closed space. Pedestrian positioning is intensively studied to obtain location with better accuracy in literature. Radio frequency based methods such as [1]–[3] use the signal strength/arrival-angle characteristics of Bluetooth or Wi-Fi signals to estimate the distance of the signal transmitter from known anchor points and then performing localization by

Manuscript received September 9, 2015; revised December 15, 2015; accepted December 16, 2015. Date of publication December 18, 2015; date of current version February 10, 2016. This work was supported in part by the Zhejiang Provincial Nonprofit Technology Research Projects under Grant 2014C31045, in part by the National Natural Science Foundation of China under Grant 61204030, and in part by the China Scholarship Council. The associate editor coordinating the review of this paper and approving it for publication was Prof. Octavian Postolache.

Q. Tian is with the College of Electrical and Engineering, Zhejiang University, Hangzhou 310027, China (e-mail: tianql@vlsi.zju.edu.cn).

Z. Salcic and K. I.-K. Wang are with the Department of Electrical and Computer Engineering, University of Auckland, Auckland 1010, New Zealand (e-mail: z.salcic@auckland.ac.nz; kevin.wang@auckland.ac.nz).

Y. Pan is with the College of Information Science and Electronic Engineering, Zhejiang University, Hangzhou 310027, China (e-mail: panyun@vlsi.zju.edu.cn).

Digital Object Identifier 10.1109/JSEN.2015.2510364

fingerprinting and trilateration/triangulation. However, these methods suffer greatly from physical environment variations and multi-path effects. Another popular alternative is to use Inertial Measurement Unit (IMU) that consists of different kinds of sensors, such as accelerometers, gyroscopes and magnetometers, to track the target with proper motion models. IMUs [4]–[6] are mounted on foot or attached to a certain part of human body collecting desired data to obtain motion information. Many methods are proposed to compensate sensor drift/error in order to enhance the accuracy and robustness of the positioning system. For instance, when acceleration along walking direction is used to estimate distance by double integration, Zero-Velocity-Update (ZUPT) [4] will reset the error accumulation of accelerometer in stance phase of walking. Apart from dedicated systems with IMUs, mobile devices, typically smartphones, become natural and ideal alternative platforms for pedestrian localization thanks to the rapid development of such devices with powerful processing capacity and integration of different sensors. Several recent works [7]–[13] have been done in this field. Step based Pedestrian Dead Reckoning (PDR) combined with step length and orientation estimation is a common strategy as it does not introduce the double-integral of accelerometer drift error into the system. The whole system can be reinforced by a fusion filter and context/map information [14], [15]. However, existing approaches are limited to and only able to perform tracking when the smartphone is carried in a very defined and constrained way during the entire walking period, which is not realistic under the PDR context. Meanwhile, [20], [21] have investigated the issue of mode recognition (i.e. ways of carrying a phone) during walking but none of them have conducted practical tracking of pedestrian involving change of mode of the smartphone. The most commonly used mode in literature is holding the smartphone in hand in front of the body [10], [12], [17], [21], which introduces great limitations and impracticalities to the developed system in real life applications.

To build a more robust tracking system, an IMU-based approach that adds identification of the mode in which the phone is carried and combines it with PDR is proposed in this paper with smartphones as the target platforms. In our previous work [23], an Enhanced PDR (EPDR) approach is proposed, which is also able to support pedestrian tracking in different modes with a typical placement of the smartphone. While this paper extends EPDR with unconstrained placement of the phone in different modes and proposes Multi-Mode

PDR (MMPDR). The main contributions of the paper are listed as follows.

1. In MMPDR, three modes during walking, i.e., holding a device in front of the body, holding and swinging freely with a hand and keeping the device in a front trousers pocket, are identified and utilized to enhance both positioning and tracking. There are few constraints on how the device is carried, thus the independence on the carrier/user is achieved.
2. Steps are detected based on the knowledge of the walking modes thus the computation effort can be reduced compared to previously reported methods.
3. A new step length model that supports users with different height, gender and walking speed is proposed, resulting with better accuracy and robustness.

The tracking is based on the assumption of the known initial position. The proposed method is implemented as a light-weight system and tested on a commercial off-the-shelf smartphone. It achieves real-time localization and tracking of the pedestrian with meter-level accuracy on long distances, without correction of position using other sensing techniques.

The remainder of the paper is organized as follows. Section II gives a brief description of PDR problem formulation and related work. Section III introduces the proposed MMPDR approach in detail. Implementation and experimental evaluations can be found in Section IV, as well as comparison with previous works. Finally, conclusion remarks and future works are presented in Section V.

II. PROBLEM FORMULATION AND RELATED WORKS

PDR systems are continuously updating a state vector S_T , typically an x - y coordinate which describes the target location in an environment from a known initial position. The position state vector is updated every time new sensor data arrive or a valid step is detected in step-based approaches. In the former one, an IMU attached to certain part of the body or mounted on the shoe provides accelerometer readings along the direction of walking and the data are double integrated to obtain the travelled distance. ZUPT [4] or self-resetting [16] algorithms are developed to compensate the accumulated error caused by sensor drift and noise. In step-detection based methods, the function describing the system is shown in equation (1) evolving from previous step position $[x_{s-1}, y_{s-1}]^T$ to the next position $[x_s, y_s]^T$ where L_s represents the length of a step and θ is the angle describing the orientation of the step in a defined coordinate plane, respectively.

$$\begin{bmatrix} x_s \\ y_s \end{bmatrix} = \begin{bmatrix} x_{s-1} \\ y_{s-1} \end{bmatrix} + L_s * \begin{bmatrix} \sin\theta \\ \cos\theta \end{bmatrix} \quad (1)$$

Accelerometer readings are continuously collected and processed in order to detect steps. Mikov *et al.* [8] and Qian *et al.* [9] calculate the magnitude of the overall 3-axis acceleration and [10] uses only one axis of accelerometer data during walking when carrying the device in a pre-defined way. In the method presented in [11], the acceleration on global z -axis, which is vertical to ground, is utilized as it only investigates the situation when the smartphone-shaped IMU is

placed in the front trousers pocket. Gaits information in the acceleration signal is detected and recognized as steps mainly based on thresholding and zero-crossing. After the detection of a valid step, the step length can be estimated based on various step length models available in the literature as expressed by equations (2) to (4). A static model [17] estimates step length as a constant relative to height and gender with h represents the height, k_1 equals to 0.415 for male and 0.413 for female in (2). This model is relatively simple and other enhancements, shown in (3) and (4), are proposed in [18] and [19] where step length is modeled using the acceleration vertical to ground while walking. The maximum and minimum value of vertical acceleration during one step, denoted by a_{max} and a_{min} , are used in (3) to calculate the step length and k_2 represents the constant value to obtain appropriate step length. While in (4), the step length is related to all samples of vertical acceleration during one step. a_i and N represent the vertical acceleration sample and the total number of samples in one step. k_3 is also a constant value used for acquiring proper length of a step. Regarding the mode in which the phone is carried, [20] investigates the mode recognition of carrying the IMU but the mode of keeping the phone-shaped IMU in pocket is not included, which is a typical mode in PDR context. Also, the mode recognition involves computationally intensive procedures of both time domain and frequency domain feature extractions and no experimental results regarding walking with different modes are presented as [20] mainly focuses on step detection.

$$L_s = k_1 * h \quad (2)$$

$$L_s = k_2 * \sqrt[4]{a_{max} - a_{min}} \quad (3)$$

$$L_s = k_3 * \sqrt[3]{\sum_{i=1}^N |a_i| / N} \quad (4)$$

Finally, the step orientation is introduced to accumulate the detected steps in the direction of walking. Gyroscope and magnetometer can be used in determining orientation as gyroscope is able to provide pitch-roll-yaw angular rotation rate and attitude of the device with respect to a reference frame and magnetometer can detect magnetic field around the device to obtain orientation like a compass. Besides, work presented in [11] uses Principal Component Analysis (PCA) to determine the axis of motion, i.e., direction of motion, in a global frame and achieves unconstrained placement of the IMU in the front trousers pocket.

A PDR system works on the basis of combining step length and orientation and the positioning accuracy of the system in indoor environment can be further improved when considering the floor plans of buildings with turn detection and map matching [24], [25].

In [21], a pedestrian navigation system is developed addressing different step modes and device poses (same as modes defined in this paper) during walking. Multilayer Perceptron (MLP) and Support Vector Machine are used as classifiers to determine the step modes (walking, running and going up/down stairs) and device poses (texting, swinging, pocket and phoning) by offline extraction of complex time domain and frequency domain features of sensor data. Also, feature vector training is required for each user before tracking.

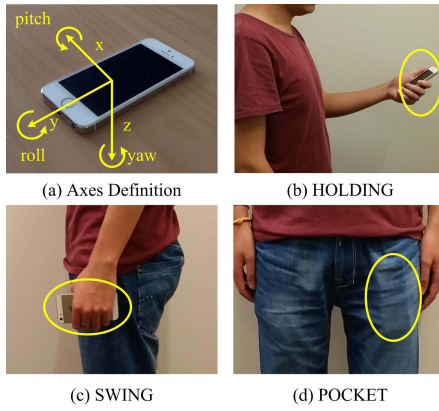


Fig. 1. Definition of mobile phone's axes and modes in MMPDR.

Nevertheless, the pedestrian tracking experiment presented in [21] is conducted in texting mode only.

To the best of our knowledge, existing works developing PDR on smartphones or using IMUs have limitations that only one or several ways of carrying the device, referred to as modes, can be supported separately and involve computationally intensive methods, such as FFT and PCA, which are not ideal under PDR context with the requirement to operate in real-time. The Multi-Mode PDR, MMPDR, presented in this paper differs to existing approaches by being able to identify the mode of carrying the phone automatically during the process of localization and tracking. The mode information is used to improve tracking accuracy while allowing phones to be carried in a more natural way. MMPDR currently supports three typical modes of carrying the device, uses a light-weight algorithm to detect the steps during walking and then uses this information to track the smartphone user in real-time.

III. MMPDR TRACKING SYSTEM

This section introduces the proposed approach with an overview first, followed by mode classification, step detection, step length estimation and orientation determination, respectively.

A. Overview

Fig. 1(a) shows the axes defined for the mobile phone. According to the placement of the device, the modes of carrying it are categorized as follows (see also *Fig. 1*): HOLDING, the user holds the phone in hand in front of the body as in *Fig. 1(b)*, SWING, the phone is held in hand and swung freely besides human body as in *Fig. 1(c)*. POCKET, the phone is placed in the pocket while walking. As there are many possible pocket placements of the phone, this paper investigates the situation of the front trousers pocket as in *Fig. 1(d)*. No further constraints on the ways how the phone is carried are imposed.

In our approach, all sensor data are collected by a customized application developed and run on an iPhone 5s with a sampling frequency of 50Hz. The built-in IMU of the smartphone is accessed using the Application Programming Interface (API) provided in Xcode sampling accelerometer and gyroscope data. Accelerometer data used are gravity

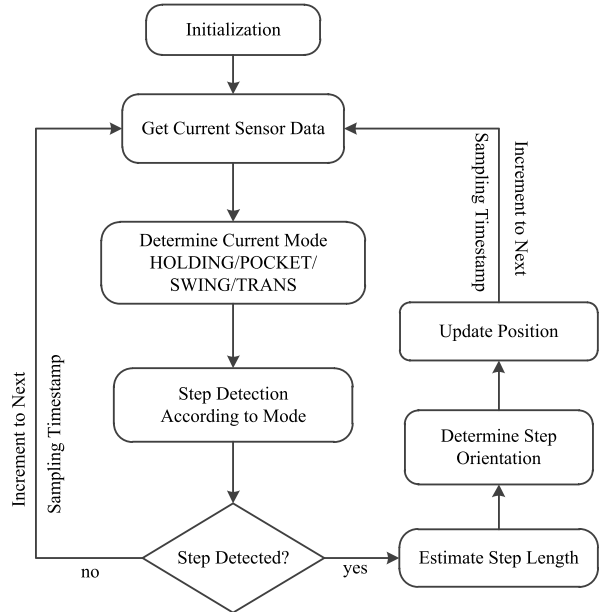


Fig. 2. Overview of MMPDR tracking system.

acceleration and user acceleration, with units in g ($*9.8m/s^2$). Gyroscope data collected are angular rotation rate and the phone's attitude in radians defining the pitch-roll-yaw angle of the phone's orientation with respect to a reference frame where the phone's x - y plane is parallel to the ground. By taking in these sensor data together with the timestamps of samples, our approach can identify different modes and employ a light-weight algorithm to accomplish the task of pedestrian tracking. *Fig. 2* gives an overview of the proposed step-based MMPDR Tracking System (MMTS). After initialization, the iteration of updating the position is triggered every time new sensor data are sampled. Upon receiving sensor data, mode identification is firstly done to determine the current mode of carrying the phone. An additional, temporary mode TRANS is introduced here, representing the transition between normal/main modes. Then, the step detection is performed according to current mode of the phone. If no valid step is detected, no further processing is required and the system waits until new sensor data arrive. Alternatively, the length and orientation of a step are estimated if a valid step is detected. These results are used to update the position of the pedestrian according to the motion model in (1). The same procedure is performed after acquiring every new reading from the sensors. The following sections describe each part of the tracking system as well as its features and advantages.

B. Mode Classification

Unlike the classification methods commonly found in literature [20], [21], which classify the modes by extracting statistical features of sensor data after every sample, the mode information in the proposed approach is determined by a Finite State Machine (FSM), shown in *Fig. 3*, that has 4 states covering all modes and transitions between modes. The three main modes (states) of the phone, i.e., HOLDING, SWING and POCKET, are bridged by the TRANS state, which corresponds to the transition between the main modes.

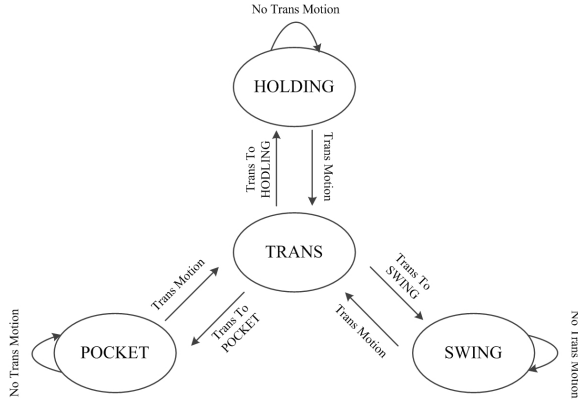


Fig. 3. Mode finite state machine.

TABLE I
PSEUDO CODE FOR MODE FSM

```

initialize current state  $S_c = \text{HOLDING}$ 
if  $S_c \neq \text{TRANS}$ 
  check for Trans Motion condition, the condition varies based on  $S_c$ 
    HOLDING: is  $r_y > R_y$  or  $r_z > R_z$ 
    SWING: is  $r_y > R_y$ 
    POCKET: is  $r_z > R_z$ 
  if Trans Motion condition is satisfied
    next state  $S_n = \text{TRANS}$ , record  $S_c$  as the mode before transition  $S_{bt}$ 
  else
    next state  $S_n = S_c$ ;
  end if
else monitor gravity during the 2-second transition window and make decision as follows afterwards to find the mode after transition  $S_{at}$ 
  if  $S_{bt} = \text{SWING/POCKET}$ 
    if Trans to HOLDING* condition is satisfied
       $S_{at} = \text{HOLDING}$ 
    else
       $S_{at} = \text{POCKET/SWING}$ 
    end if
  else
    if Trans to SWING# condition is satisfied
       $S_{at} = \text{SWING}$ 
    else
       $S_{at} = \text{POCKET}$ 
    end if
  end if
end if
  
```

* *Trans to HOLDING*:
any sample during the 100-sample window meets the following
($g_y < -GH_y$ and $g_z < 0$) or ($g_z < -GH_z$ and $g_y < 0$)
Trans to SWING:
any sample during the 100-sample window meets $\text{abs}(g_x) > GS_x$
and all samples of $g_z < GS_z$

The pseudo code presented in Table I summarizes the process of mode classification. During initialization of MMTS, the FSM state is initially set to HOLDING with reasonable assumption that the implemented smartphone application requires certain user interaction to start the system. Afterwards, the FSM either stays in a main mode state, when no transition motion is detected, or is otherwise triggered to TRANS state.

Transition motion is characterized by the orientation change of the phone and is detected through monitoring the angular rotation rate of the phone in y-axis and z-axis, by thresholding. As can be seen in the pseudo code, the condition of

TABLE II
ROTATION RATE MONITORED FOR TRANSITION DETECTION

Mode	Axis of Rotation Rate Monitored
HOLDING	y-axis and z-axis
SWING	y-axis
POCKET	z-axis

Trans Motion is satisfied differently according to the current state of the FSM. The rotation rate monitored in each mode is also tabulated in Table II. For HOLDING mode, the orientation of the phone is relatively stable so both y-axis and z-axis rotation rate, r_y and r_z , are monitored. While for SWING mode, only r_y is monitored as the phone rotates around z-axis in the regular motion during walking in this mode. Similarly in POCKET mode, only r_z is monitored to detect the transition motion. R_y and R_z represent the y-axis and z-axis rotation rate threshold used to detect a transition motion.

When the monitored rotation rate exceeds the threshold, the transition motion is identified and the FSM state will immediately change into TRANS state. The state before transition motion is recorded as S_{bt} at the same time. The TRANS state is kept throughout a two-second window and corresponds to a 100 sample interval. During the time window, features in 3-axis gravity acceleration, g_x , g_y and g_z , are monitored to determine which state the phone is transiting into, namely S_{at} . The gravitational acceleration in HOLDING is unique as gravity is split on y-axis and z-axis, while gravity mainly resides on x-axis for SWING mode. The analyses on y-axis and z-axis gravity thresholds in HOLDING mode, GH_y and GH_z can be found in Section III-C.

However, for POCKET mode, the gravity characteristic is not obvious since the position of the phone inside a trousers pocket is unpredictable due to various shapes of pockets and fabric of the trousers. Considering the fact that there are only two possible modes the phone can transit into with the knowledge of the mode before transition, the condition *Trans to HOLDING/SWING/POCKET* in Fig. 3 can be simplified as described in the pseudo code in Table I where only *Trans to HOLDING/SWING* is evaluated. For the *Trans to SWING* condition, the absolute value of x-axis gravity g_x is used to support swinging the phone both in left and right hand. The extra constraint on g_z is used for better differentiation between transition into SWING or into POCKET from HOLDING mode. A positive value of g_z indicates the phone's screen is facing the ground (the value is negative in HOLDING mode) so its reading should not exceed a positive threshold when transition to SWING from HOLDING mode. Details of parameters tuning of the algorithm presented in Table I can be found in Section IV-A.

The above-implemented FSM used to determine the mode possesses great scalability as the FSM can be further extended to support additional modes of carrying the phone, all bridged by the TRANS state.

C. Step Detection

Detecting steps accurately is vital and will significantly influence the positioning performance of the system. As can be

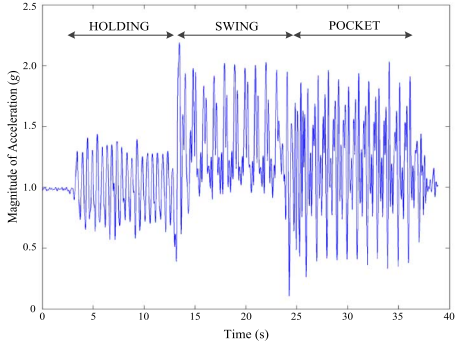


Fig. 4. Magnitude of acceleration in different modes.

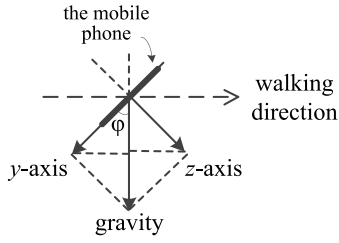
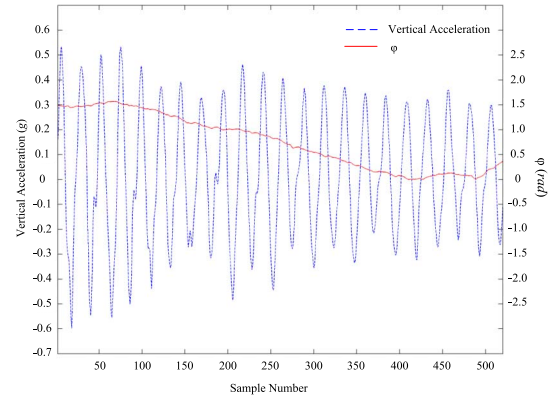


Fig. 5. Analysis in the HOLDING mode.

seen from *Fig. 4*, the magnitude of overall 3-axis acceleration with gravity included shows distinctive features in different modes and is hard to find a unified way to detect steps by simple thresholding. In the proposed approach, the steps are detected with knowledge of the current mode. Based on the recognition of current mode, the acceleration data used in step detection are vertical, y-axis and z-axis user acceleration in HOLDING, SWING and POCKET mode, respectively, as summarized in Table III.

In developing the light-weight step detection scheme, accelerometer data of gravity acceleration and user acceleration are used. Bertram and Ruina [22] pointed out that human step frequency is in the range of 0.5-5Hz so the raw user acceleration data sampled at 50Hz is firstly smoothed by a low pass filter with cut-off frequency at 5Hz.

For the HOLDING mode, the vertical user acceleration is in the direction vertical to ground and the accelerometer data from a single axis are insufficient to obtain vertical acceleration. It is observed that different people tend to hold the phone differently with varying angles between the phone's x-y plane and the horizontal plane. A cross-section of the plane vertical to ground and parallel with walking direction is illustrated in *Fig. 5*. The vertical acceleration is calculated in the way that the angle φ is firstly found out utilizing the gravity acceleration of the phone in y and z axes as shown in equation (5). The vertical user acceleration, denoted by a_{uv} , is then calculated by combining the components of y-axis and z-axis user acceleration in vertical direction as in equation (6), where g_y , g_z , a_{uy} , a_{uz} denotes the readings of gravity acceleration on y and z axes, as well as user acceleration on y and z axes, respectively. The scheme possesses a favorable feature that it works accurately for people with different preferences in holding the phone and is also immune

Fig. 6. Vertical acceleration and φ in HOLDING mode.

to angle changes in a continuous walk. As shown in *Fig. 6*, the correct vertical acceleration can be obtained when the angle φ varies between 0 to $\pi/2$.

$$\varphi = \text{atan}(\text{abs}(g_z/g_y)) \quad (5)$$

$$a_{uv} = a_{uz} * \sin\varphi + a_{uy} * \cos\varphi \quad (6)$$

After the above analysis in HOLDING mode, the threshold used in TRANS to HOLDING condition in Table I can be explained as follows. Referring to *Fig. 5*, gravity is split in y-axis and z-axis, the value on each of these two axes is equivalent when φ is 45° and equals to $0.707 (\sqrt{2}/2)$ in an ideal case. However, the y-z plane of the smartphone may not be ideally perpendicular to the ground and gravity will also split on x-axis due to variations in human posture in real life situation. In order to strengthen the robustness of the mode recognition against variations, HOLDING mode should be recognized even if the phone is rotated around y-axis by an angle of η . In rare conditions where user is holding the phone in a slightly tilted angle (around y-axis), the magnitude of gravity component is reduced on y-axis and z-axis, which should also be taken into consideration when setting the gravity thresholds GH_y and GH_z in Table I. The relation of η , GH_y and GH_z is expressed in equation (7). In general postures when people interact with the smartphone in HOLDING mode, η should not exceed 30° to allow user interacting with the phone. In order to recognize HOLDING mode when φ varies between 0 to $\pi/2$, the thresholds GH_y and GH_z should be equivalent since the dominant gravity component is along y-axis and z-axis when $\varphi < 45^\circ$ and $\varphi > 45^\circ$, respectively. Therefore, $GH_y = GH_z = 0.65$ when η equals to 30° is selected.

$$\eta = \text{arctan}(\sqrt{1 - GH_y^2 - GH_z^2/GH_z}) \quad (7)$$

The step detections in all three modes are based on finding the peak value in the corresponding filtered and processed user accelerations (Table III). For HOLDING and POCKET mode, only positive peak is detected while for the SWING mode, both positive and negative peaks are detected since the phone experiences the motion similar to a pendulum. The basic idea of detecting a valid step is that the absolute value of the peak is greater than a given threshold. However, the following

TABLE III
ACCELERATION USED IN STEP DETECTION IN DIFFERENT MODES

Mode	Type of User Acceleration
HOLDING	Vertical to ground
SWING	y-axis
POCKET	z-axis

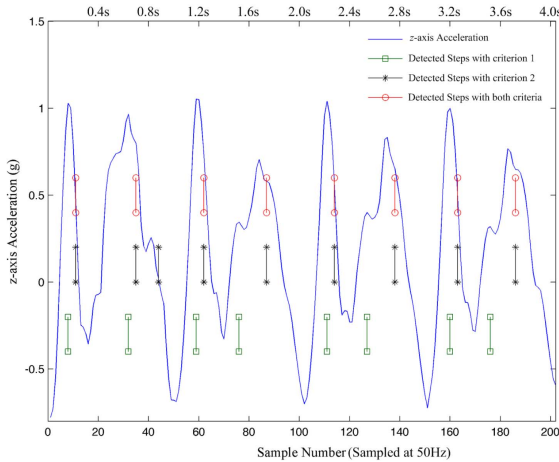


Fig. 7. Performance of additional criteria in step detection.

additional criteria are also considered in our algorithm to achieve better performance.

Criterion 1: Maximum step frequency is 5Hz [22] so there is a minimum 0.2s time interval between two consecutive steps. Every time a valid peak is found, its timestamp is compared to the timestamp of the previous valid step, making sure that the minimum time interval between steps is satisfied.

Criterion 2: False peaks still exist in the filtered signal and they often appear before the true peak corresponding to a valid step. Thus, a False Peak Rejection (FPR) mechanism is added. After detecting a positive/negative peak, no negative/positive peak should be identified in the following n_{fpr} acceleration samples where n_{fpr} is the size of the FPR window in number of samples.

Fig. 7 shows the performance of the two criteria when detecting steps in POCKET mode using the z-axis user acceleration. The threshold is set to $0.2g$ and $n_{fpr} = 3$. When only criterion 1 is applied, the positive peak above threshold is recognized as a step as long as the 0.2s time interval is satisfied. Meanwhile, false peaks are rejected when FPR in criterion 2 is utilized but one extra step is identified. By combining both criteria, steps are detected on true peaks corresponding to a step and a more accurate result is achieved with a consistent delay of 3 data samples after the peak for all valid steps.

After detecting valid steps, the proposed approach records the variable of step frequency indicating the number of steps per second. During initialization, the frequency is set to zero. The frequency is obtained as the reciprocal of the time interval between two consecutive steps. If no steps have been detected for 2 seconds, corresponding to a minimum step frequency of 0.5Hz, the variable is then reset to zero. Therefore, after

detecting a valid step, the step is interpreted as the initial step from the motionless state to walking mode if the step frequency is found to be zero. It is also an indicator about the motion state of the tracking target, i.e., standing still or walking.

It should be noted that valid steps exist during the two-second TRANS period but the accelerometer data are ambiguous for step detection since the acceleration data are corrupted during transition motion. As a result, no step detection is performed during the transition period and the steps in TRANS mode are compensated after transition finishes. Based on the assumption that before and after the transition, the subject maintains the same behavior of either walking or being in motionless state, the number of steps compensated during the transition period N_c is approximated by the product of the interval of transition t_t and the last updated step frequency before transition f_s followed by a *round* function, rounding to the nearest integer as shown in equation (8).

$$N_c = \text{round}(t_t * f_s). \quad (8)$$

D. Step Length Estimation

Many models of step length are proposed previously in literature and have been introduced in Section II. While in this paper, a new model is proposed to estimate the step length. Bertram and Ruina [22] investigated 12 subjects on multiple walking speed and step frequency relationship. By analyzing its result data, it is deduced that step length L_s has approximately a square root relation with step frequency. By combining other models, the proposed step length model relative to height, gender, and step frequency is presented in equation (9) where k is a constant and tuned to 0.3139 for male and 0.2975 for female, h is the height of the subject and the units of step length is in meters. The rationale for the setting of k can be found in Section IV-C. The calculated step frequency will affect the accuracy of the model. Although frequency domain analysis techniques such as FFT are able to obtain a steady step frequency value, the proposed approach is strengthened by a less computationally intensive FPR mechanism in step detection. Therefore, the step frequency obtained will be more stable and not influenced by the false peaks in acceleration for more accurate step length estimation.

$$L_s = k * h * \sqrt{f_s} \quad (9)$$

For the initial steps from motionless to walking, f_s cannot be calculated since only one step timestamp is available. So a constant step length according to (2) is set as the initial value. As for the compensated steps, the step frequency used in calculating the number of compensated steps is also used for estimating the length of compensated steps. The accuracy of the model and comparison with previous models are presented in Section IV-C.

E. Orientation Determination

Orientation helps to accumulate steps in the correct direction to form a path indicating the walking track. In the proposed approach, orientation is determined by the yaw data from

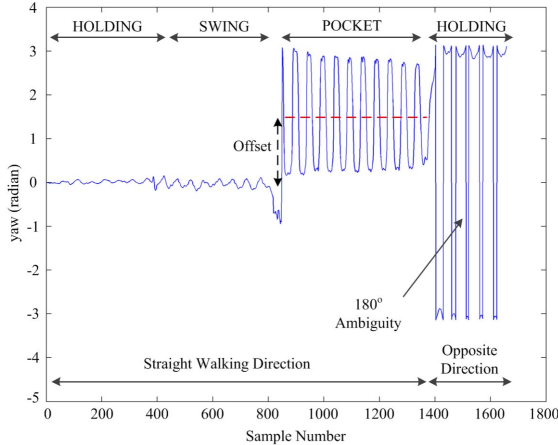


Fig. 8. Example of yaw data in different modes.

the phone's attitude information, which indicate the angle turned around the phone's z -axis and the value is in range $(-\pi, +\pi]$. Fig. 8 presents an example of yaw data in different modes when walking in a straight direction and the last part in HOLDING mode illustrates the 180° ambiguity issue in opposite direction for better understanding of the following analysis.

For HOLDING mode, the yaw data are valid and can be directly used as the θ needed for updating position in (1) when the phone is pointing to the same direction of walking. The attitude of the phone is relatively steady during walking and making a turn also corresponds to an equivalent change in the value of yaw data.

While for SWING and POCKET mode, the yaw data obtained from the sensor need to be processed to get the accurate orientation of walking.

It should be noted, oscillation in yaw data is introduced as the attitude of the phone is coupled with the motion of hand and leg in SWING and POCKET mode, respectively. For SWING mode, the oscillation is slight as the phone experiences the motion similar to a pendulum and the attitude change is minor during the motion. Meanwhile, the oscillation is more significant in POCKET mode when the phone rotates with the motion of the leg. In order to remove the oscillation, an averaging technique is applied to the yaw data within the duration of the step. To keep consistency for all modes, the averaging scheme is applied to HOLDING mode as well to calculate the orientation of the step from the recorded yaw data. Further, to achieve more accurate performance under POCKET mode, the yaw data are averaged every 2 steps since the phone is put in one side of the trousers pocket with a recurring feature every 2 steps. If averaging yaw data is performed every step, the result orientation would fluctuate around the true direction and the path may get serrated. In addition, while performing the averaging procedure, the 180° ambiguity issue would lead to erroneous result when directly averaging the raw data. Thus an extra calibration process is added to solve the ambiguity and it is outlined in the pseudo code in Table IV where ω_i is an array holding temporary values during processing, average is the function

TABLE IV
PSEUDOCODE FOR YAW DATA CALIBRATION

```

Given an array of raw yaw data  $yaw\omega_r$  with  $j$  samples
for  $l = 1 : j$ 
    if( $\omega_r(l) < 0$ )
         $\omega_r(l) = \omega_r(l) + 2*\pi$ 
    else
         $\omega_r(l) = \omega_r(l)$ 
    end if
end for
if(average( $\omega_r$ ) >  $\pi$ )
     $O_c = \text{average}(\omega_r) - 2*\pi$ 
else
     $O_c = \text{average}(\omega_r)$ 
end if

```

getting the numerical average of an array and the calibrated average value of the array is obtained as O_c .

The offset in the yaw data can be observed after the oscillation is removed by averaging. An example is illustrated in Fig. 8 with red dashed line, indicating the offset in POCKET mode. The different preferences of holding the phone in SWING mode and distinctive placements of the device in POCKET mode are reflected in varying values of the offset. To address the issue, an Adaptive Offset Compensation (AOC) scheme is developed, making the proposed approach capable of correct tracking for different targets with no constraints in both SWING and POCKET mode.

The idea of AOC scheme is to train a specific offset for compensation using the yaw data collected within the first few steps after transition into SWING/POCKET mode, referred to as training stage. It is assumed the target to be tracked maintains the direction of walking during transition and the training stage, both having the same direction with the last valid step before transition. In the implementation of the AOC scheme within the tracking system, correct direction of walking is firstly obtained from yaw data as the phone is initially in HOLDING mode. The AOC process takes place every time a transition is made into SWING/POCKET mode and is presented in the pseudo code in Table V where avg_cali represents the process of the averaging scheme to get step orientation from an array of yaw data with necessary calibration as in Table IV to resolve the 180° ambiguity. Firstly, the last recorded step orientation before transition, O_b , is saved as the baseline for offset training. For SWING mode, the first calculated M_{SWING} step orientations using the raw yaw data equal to the combination of step orientation baseline and the introduced offset. Therefore, the trained offset is obtained as the difference between the average orientation of the M_{SWING} steps and O_b . The offset training in POCKET mode has similar processing procedures except the following two features: 1) The step orientations are calculated every two steps. 2) The orientation of the phone may change right after putting it into pocket and will maintain a steady attitude afterwards. As a result, the orientations calculated for the first M_{omit} steps after transition into POCKET mode are omitted.

After the offset training stage, the trained offset is used for steps afterwards, compensating the offset introduced in SWING/POCKET mode. The scheme is adaptive as the

TABLE V
PSEUDOCODE FOR ADAPTIVE OFFSET COMPENSATION

```

Record the step orientation of the last valid step before transition as  $O_b$ 
if the mode after transition is SWING
    initialize SWING offset training array  $SA$ 
    for the  $M_{SWING}$  steps after transition do for every step
        record yaw data during the step as  $\Omega_s$ 
        calculate the step orientation with offset included
             $O_{t,s} = avg\_cali(\Omega_s)$ 
            add  $O_{t,s}$  in  $SA$ 
            clear  $\Omega_s$ 
    end for
    trained SWING offset  $O_{SWING} = avg\_cali(SA) - O_b$ 
    for steps afterwards, record yaw data during every step as  $\omega_s$ 
    the step orientation  $O_{s,s} = avg\_cali(\omega_s) - O_{SWING}$ 
end if
if the mode after transition is POCKET
    initialize POCKET offset training array  $PA$ 
    for the  $M_{POCKET}$  steps after transition, omit the first  $M_{omit}$  steps, then do for every two steps
        record yaw data during the two steps as  $\Omega_p$ 
        calculate the step orientation with offset included
             $O_{t,p} = avg\_cali(\Omega_p)$ 
            add  $O_{t,p}$  in  $PA$ 
            clear  $\Omega_p$ 
    end for
    trained POCKET offset  $O_{POCKET} = avg\_cali(PA) - O_b$ 
    for steps afterwards, record yaw data during every two steps as  $\omega_p$ 
    the step orientation  $O_{s,p} = avg\_cali(\omega_p) - O_{POCKET}$ 
end if

```

trained offset is able to adapt to arbitrary features of pedestrians with different preferences in keeping the device in SWING/POCKET mode. Besides, the actual orientations of steps used in tracking the pedestrian during offset training stage in both modes equal to the value of O_b .

As for the orientation of the compensated steps, the step orientation used is the same as the last valid step detected before transition since the yaw data can also be corrupted during transition motion.

IV. EVALUATION

This section presents the experiment setup, parameters tuning of MMTS and evaluations of the system in terms of mode classification, step length estimation and tracking of pedestrians.

A. Experiment Setup & Parameter Tuning

To carry out experiments, an application implementing the MMTS is developed and run on an iPhone 5s. Also, all sensor data, sampled at 50Hz, are recorded for more comprehensive offline analyses. In realizing MMTS, the tuning and rationales of parameter selections are detailed as follows.

In the mode classification algorithm (Table I), the threshold of gravity acceleration used in recognizing HOLDING mode is 0.65 for both GH_y and GH_z . As analyzed in Section III-C, a 30-degree rotational margin around y-axis of the phone is allowed in HOLDING mode. For recognition of SWING mode, the x-axis and z-axis threshold GS_x and GS_z is set to 0.9 and 0.4, respectively. For GS_x , it can be set to 1 in ideal case, i.e., gravity falls solely on x-axis. In practical implementation, the threshold is set to 0.9,

allowing a 26-degree rotational margin around y-axis. Within the margin, SWING mode can be correctly recognized and the variations among different people are accommodated. Regarding the rotation rate thresholds in detecting transition motion, namely R_y and R_z in Table I are set to 3rad/s and 5rad/s, respectively. Details of these two parameter selections can be found in Section IV-B.

In step detection algorithm of MMTS, the FPR window size n_{fpr} equals to 3 samples in POCKET mode and 6 samples in HOLDING and SWING mode. These values are selected by considering the maximum human step frequency of 5Hz [22], which corresponds to 10 samples at 50Hz sampling rate. In POCKET mode, the acceleration signals have a feature where false peaks and peaks with minimum amplitude in one period follow very closely to the true peaks as shown in Fig. 7. A large value of n_{fpr} will result in the true peak corresponding to a step being rejected. Therefore, n_{fpr} value in POCKET is set to 3 samples to remove small fluctuations close to the true peaks. This is the maximal possible value without causing true peaks being rejected and at the same time avoids local false spikes close to the true peaks. In HOLDING and SWING mode, the periodic acceleration signal coupled with human motion is similar to sinusoid waves corrupted with possible false spikes in the middle of two steps. A small value of n_{fpr} will have no effect in rejecting false peaks in HOLDING/SWING mode. Therefore, the value of n_{fpr} is set to 6 samples, which is sufficiently long to remove the misleading fluctuations without rejecting the true peaks. The above settings of n_{fpr} correspond to a sampling frequency of 50Hz and should be changed proportionally with different sampling rate.

The parameter setting in orientation determination algorithm includes the number of steps used in offset training phase of AOC scheme. In MMTS, the pedestrian is assumed to maintain the direction of walking during transition and the training stage, both having the same direction with the last valid step before transition. The number of steps used in training stage should be chosen to minimize the time needed for offset training and at the same time avoid relying on a single orientation value by averaging in several steps. For SWING mode, the step orientation of three steps, i.e., $M_{SWING} = 3$, are averaged to obtain the trained offset. While the orientations of the first two steps when transitioning into POCKET mode are omitted since the attitude of the phone may change right after putting into pocket. The following four steps are used to train the offset since the orientation in POCKET mode is calculated on a two-step basis. Therefore, $M_{POCKET} = 6$ and $M_{omit} = 2$.

B. Mode Classification

By using the parameters presented in Section IV-A, experiments were conducted to evaluate the performance of the mode classification algorithm with 17 participants in different age groups from 22 to 65 years old. Everyone took an 80-meter straight walk and the mode of carrying the phone was changed freely during the experiment. The subjects were only informed of the three modes in keeping the device and no additional information was provided.

TABLE VI
EXPERIMENTAL RESULT OF MODE CLASSIFICATION

Mode	HOLDING	SWING	POCKET
Classified as HOLDING	96.88%	5.26%	3.57%
Classified as SWING	0	89.48%	3.57%
Classified as POCKET	3.12%	5.26%	92.86%
Transition Motion Missed		7.55%	
False Trigger into TRANS mode		1.89%	

In the experiment, a total number of 106 transitions between pairs of the three modes were made and the results by applying the proposed mode classification approach are summarized in Table VI. 8 transition motions, 7.55% of total transitions, are missed in situations where the monitored rotation rate does not surpass the threshold. Despite the wide age range of the participants, the rotation rate is proved to be a reasonable indication for detecting transition motion. In the missed transition motion, the maximum rotation rates in y -axis and z -axis are in range of 2.47-2.90rad/s and 3.79-4.77rad/s, respectively.

For the detected transitions, the accuracy of classification in percentage is listed in Table VI, all achieving over 89% accuracy. The HOLDING mode is recognized with highest accuracy as the gravitational acceleration feature in HOLDING mode is unique. Also observed from the results, 2 false transitions are triggered when no transition motion is performed. The false trigger rate is as low as 1.89% since the rotation rate in the monitored axis in each mode is stable during regular walking motion. By using the defined thresholds in the approach, a detection rate of 92.45% is achieved while false trigger into TRANS state is effectively avoided.

C. Step Length Estimation

In order to obtain the value of the constant k in (9) with better step length estimation accuracy for subjects with varying height, gender and walking speed, experiments are conducted and the performance of the step length model is compared with existing models in (2) - (4) as well. Since the models in (3) and (4) use the vertical acceleration to estimate the step length, experiments and comparisons are carried out in the HOLDING mode. The acceleration data and timestamp are recorded by the application.

Ten subjects, five males and five females with height in range of 1.56m-1.83m, participated in the experiment. Everyone was asked to perform three independent walks in a 28m corridor with slow, moderate and fast walking speed, respectively. Then, different step length estimation methods are applied to each data set to calculate the distance travelled. As k_1 is already defined, the constants in other models, k , k_2 , k_3 , are tuned to a value so that the average of all estimated distances in each model is 28m, i.e., the real distance. The method applied in tuning the constants uses a similar approach as in [8] by optimization analysis based on experiment data, achieving minimum error performance for all data sets. In this way, k is tuned to 0.3139 for male and 0.2975 for female subjects. The results of estimated travelled distances for each model according to (2)-(4) and (9) are summarized in Table VII where minimum, maximum, median

TABLE VII
STEP LENGTH MODEL COMPARISON

Distance (m)	Minimum	Maximum	Median	STD
Eq. (2)	22.19	36.31	26.92	3.58
Eq. (3)	22.70	33.59	28.04	2.69
Eq. (4)	22.64	32.04	28.39	2.73
Eq. (9)	24.56	32.27	27.96	2.30

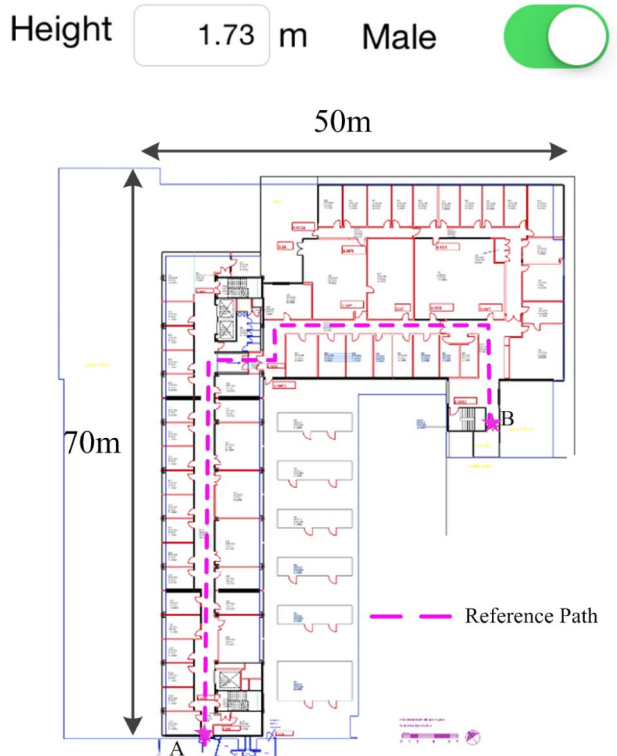


Fig. 9. Screenshot of the developed application.

value of estimated distance and standard deviation (STD) are presented.

A common feature revealed in the test data is that the step count for each individual decreases when walking speed increases. With a faster walking speed, the step frequency is also higher and this proves that step length is proportional to the step frequency. Also, variations in walking speed are observed since different walking speeds of slow, moderate and fast are determined by each subject. The time taken in the 28m walk varies from 14.9s to 38.76s among ten subjects, which corresponds to an average walking speed range of 0.722m/s to 1.879m/s. As can be seen from the results of estimated distances in Table VII, the median values of all methods are close to the real distance, providing an acceptable performance in general cases. While for STD, static method using (2) is obviously greater than the other methods. The static model estimates the step length as a fixed value for every subject but the step count in all experiments ranges from 32 to 54 steps for the same travelled distance of 28m, resulting in large variations in estimated distance. Of all the models, the proposed one estimating step length according to (9) achieves the minimum STD value, indicating the robustness of accurate



Fig. 10. Tracking of pedestrians results in single mode. (a) HOLDING. (b) SWING. (c) POCKET.

step length estimation for subjects with varying height, gender and walking speed. In addition, the proposed model is also less computationally expensive compared to (3) and (4). It only needs two timestamp samples of detected steps in estimation, sparing the effort to record or monitor all the acceleration data within one step.

D. Tracking of Pedestrians

Multiple tracking experiments were conducted to evaluate the tracking performance of MMTS. Fig. 9 is a screenshot of the developed application implementing MMTS. The figure in the application illustrates the layout of Level 2 of Science Center Building, the University of Auckland, with an area of 70m*50m. The dash line on the map outlines the reference path travelled by the subjects in the experiment from point A to point B with a total distance of 96.33m and the duration of the walking is about 90 seconds. Since the step length model in the proposed approach is relevant to the height and gender of the target to be tracked, these information can be adjusted using the textbox and switch above the map for different test subjects, whose default values are set to height 1.73m and gender of male. Similar to [12], position and heading errors are measured by comparing the tracking result with the reference path in quantifying the performance of MMTS. Position error is obtained by calculating the distance between reference position and user location at every meter of the travelled distance. Heading error is evaluated by comparing the step orientation with the direction of reference path for every step. Therefore, the average/median position/heading errors of a path (values presented in Table VIII to Table X) are numerical average/median of all measured position/heading errors along the path.

Experiments testing the MMTS are firstly carried out tracking a male subject with height 1.73m in single mode for the walking path from *A* to *B* along the corridor. The walking

TABLE VIII
TRACKING STATISTICS – SINGLE MODE

Mode	HOLDING	SWING	POCKET
Tracking Path	<i>Fig 10(a)</i>	<i>Fig 10(b)</i>	<i>Fig 10(c)</i>
Actual Step Count	131	128	128
Total Estimated Step Count/Percentage	131/ 100%	127/ 99.22%	126/ 98.44%
Total Estimated Distance Traveled (m)	96.37	94.76	93.31
Maximum/Median Heading Error (deg)	14.23°/ 1.96°	14.8°/ 4.63°	10.58°/ 3.16°
Average Position Error (m)	0.75	1.33	0.71
One Iteration Maximum Processing Time (ms)	14.2	12.3	13.6

path is plotted on the screen in real-time during walking. To distinguish the path walked in different mode, different colors are used for drawing the path with red for HOLDING, blue for SWING and green for POCKET mode, respectively. The tracking results produced by the smartphone application are illustrated in *Fig. 10* in all three modes and the tracking paths clearly reflect the true path shown as the dashed line in *Fig. 9*. Table VIII also tabulates quantified results of the tracking. As can be seen, high step detection rate is achieved with a minimum percentage of 98.44%. The travelled distance estimated also achieves an average of 98.43% accuracy, confirming the precision of the step length model in practice. The position errors for all three modes and the averaged values are also visualized in *Fig. 11*. The average position error remains below 0.6m in the initial path of a 45-meter straight line and then rises when making turns and the maximum value remains below 2.5m during the whole tracking period.

Moreover, multiple walking experiments in mixing all three modes defined in MMTS are conducted with different subjects to show the effectiveness of the proposed approach when the

TABLE IX
TRACKING STATISTICS – MULTI-MODE

Subject	S1	S2	S3	S4	S5
Height/Gender	1.65m/Female	1.60/Male	1.59m/Female	1.74m/Male	1.73m/Male
Tracking Path	<i>Fig. 13(a)</i>	<i>Fig. 13(b)</i>	<i>Fig. 13(c)</i>	<i>Fig. 13(d)</i>	<i>Fig. 13(e)</i>
Actual Step Count	140	140	140	130	133
Total Estimated Step Count/Percentage	139/99.3%	141/100.71%	137/97.9%	124/95.4%	127/95.5%
Total Estimated Distance Travelled (m)	96.70	95.07	91.43	92.86	96.03
Maximum/Median Heading Error (deg)	17°/3.41°	15.98°/5.00°	13.52°/3.58°	11.22°/2.97°	9.91°/1.94°
Average Position Error (m)	1.34	2.00	0.83	1.01	0.30
Trained SWING Offset (rad/deg)	-0.025/-1.43°	-0.050/-2.87°	0.052/2.98°	-0.082/-4.70°	-0.104/-5.96°
Trained POCKET Offset (rad/deg)	0.692/39.67°	-0.12/-6.88°	0.758/43.45°	-0.985/-56.46°	1.95/111.78°
One Iteration Maximum Processing Time (ms)	6.8	7.7	11.6	14.7	7.3
					13.9

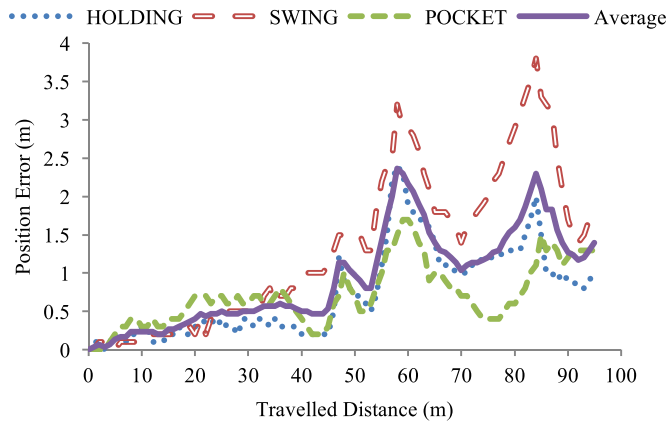


Fig. 11. Position error in single mode.

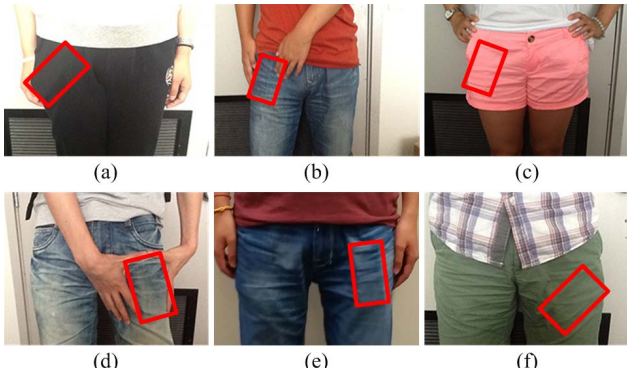


Fig. 12. Different positions of phone in pocket. (a) Subject 1. (b) Subject 2. (c) Subject 3. (d) Subject 4. (e) Subject 5 jeans trousers. (f) Subject 5 casual trousers.

mode of carrying the phone can be changed with unconstraint placement. Trousers photos of different subjects are shown in *Fig. 12* including casual, jeans and sport ones, and the smartphone inside the pocket is sketched by the red rectangular. *Fig. 12(e)* and *(f)* are the same subject wearing different trousers. The tracking paths as well as quantified results of the walking are presented in *Fig. 13* and Table IX.

Fig. 13 presents the path plotted while the subjects with corresponding trousers as shown in *Fig. 12(a)-(f)*. Each path, *(a)-(e)*, includes all three modes of the phone identified by

different colors of the path. Experiment *(f)* is conducted to test its performance with different trousers of the same target so it only consists of two modes, i.e., HOLDING and POCKET mode. The result drawn by the application clearly outlines the true path walked and the multi-colored path also proves the accurate performance of the mode classification method.

Meanwhile, Table IX summarizes numerical results during the tracking. The proposed MMTS achieves high accuracy on detected steps and travelled distance, with an average performance of 97.75% detected steps and 97.83% travelled distance, respectively. For different subjects, the system is able to track them properly with the proposed AOC scheme. For results *(a)-(e)*, the trained offset for SWING and POCKET mode is presented. For the SWING mode, the compensated offset varies slightly among subjects, within the absolute value of 6°, as not much difference is observed in the motion when a person walks with the phone swinging in hand. While for POCKET mode, the offset differs a lot due to different orientation of the phone inside a pocket. Without offset compensation, the walking path would easily get diverged and lead to significant position error. For result *(e)* and *(f)*, the offsets trained are also different for the same subject. It is observed in the experiments that the compensated offset for POCKET mode is relevant to the orientation of the phone inside the pocket. Also, the proposed AOC scheme works well even when the phone is put in the rear trousers pocket. The scheme is able to compensate arbitrary offset after the orientation of the phone changes as long as the pedestrian maintains the same orientation during the offset training period.

Of all the paths of walking presented in both *Fig. 10* and *Fig. 13*. The source of position error mainly comes from two factors. The first is the sensor drift in gyroscope, results in the heading error of the path. Heading errors can be easily observed in the latter part of all the paths. Referring to *Fig. 10*, the sensor drift is more obvious in SWING mode. The reason is that the phone rotates around its z-axis more significantly together with the hand motion in SWING mode and results in the accumulated error in yaw angle growing faster. As yaw angle is used in determine the orientation of walking, the error is then visible in the plotted path. The sensor drift also influences the AOC scheme when the mode of the smartphone changes. For instance in *Fig. 13(a)*, the sensor drift can be observed in the HOLDING mode before

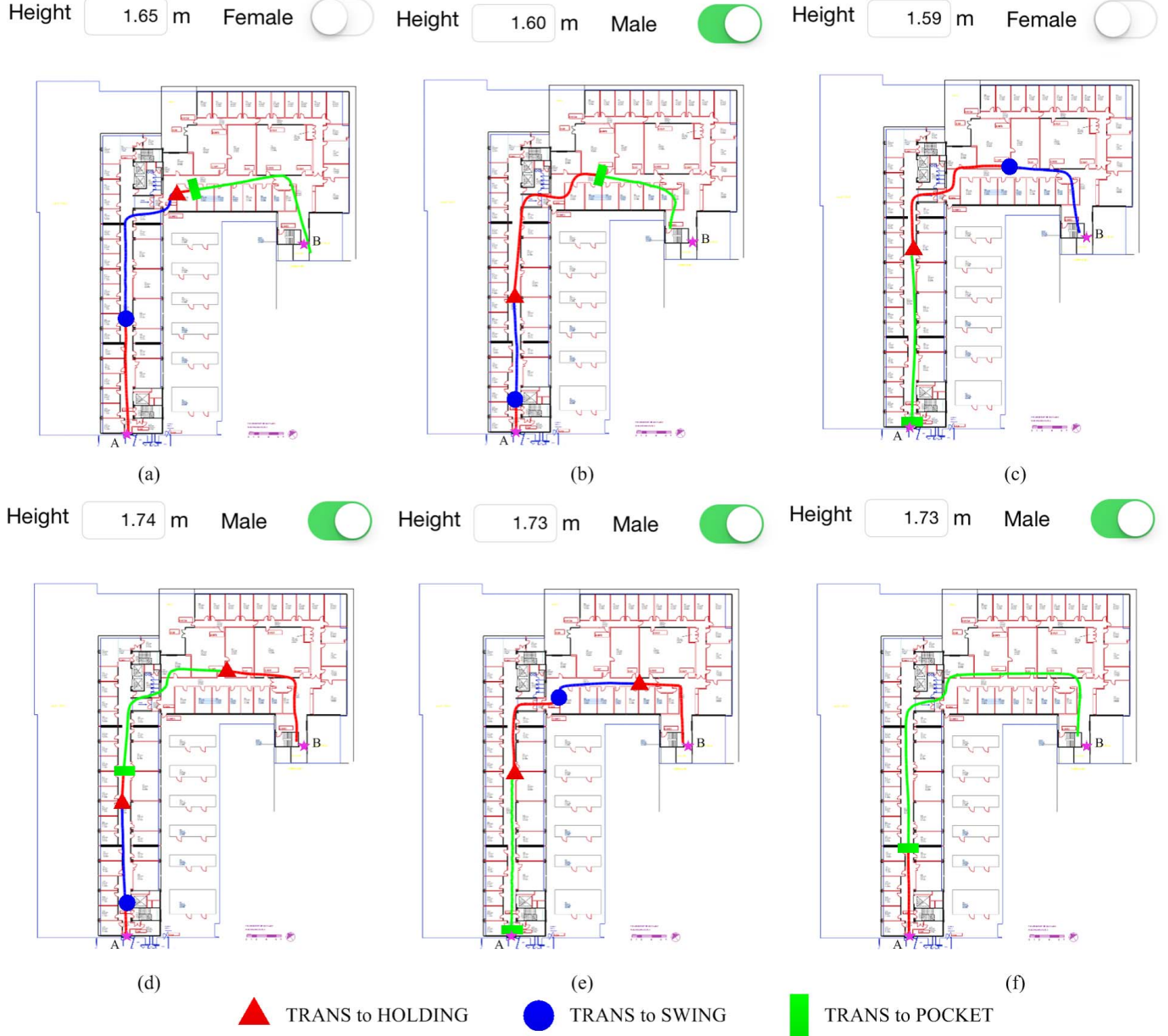


Fig. 13. Tracking of pedestrians results in multi-mode. (a) Subject 1. (b) Subject 2. (c) Subject 3. (d) Subject 4. (e) Subject 5 jeans trousers. (f) Subject 5 casual trousers.

transition into POCKET mode. After the transition is made, the drift also affects the offset training period. Thus the error still exists in the path afterwards. The other source of error comes from undetected steps. As in the path before the last turn in *Fig. 11(c)*, the plotted track is shorter than the real path due to undetected steps. In the MMTS, one undetected step will influence itself as well as the step right after it. On one hand, the step that is not detected will not have a corresponding path in the walking track. On the other hand, it will also lead to an error in the calculated step frequency for the next step. The step frequency will be underestimated as the time interval actually corresponds to two steps. Then, the step length will also be underestimated. Of the two sources of error, heading error is the dominant one as the position error would grow quickly if an erroneous heading is estimated.

Considering the performance of the above presented results of MMTS in single mode and multi-mode, Table X gives comparisons with similar previous works developed with IMU or smartphones. The result of [11] is the one obtained with rotational method without any PCA processing, which is similar in principle with MMTS. Some results are not available in the referred works and are presented as *NA*. To give a fair comparison among different works with varying total length of the experiment track, the distance and average position accuracy are reported in percentage with respect to the overall tracking distance. Seen from the table, these two performances, i.e., distance and position accuracy, of all works are comparable, all achieving above 97% accuracy in distance estimation and 98% in position accuracy. Regarding heading error, both median and mean heading errors of MMTS are listed for

TABLE X
PERFORMANCE COMPARISON

	Heading Error (deg)		Distance Accuracy	Average Position Accuracy
	Median	95 th percentile		
[11]	13.7°	19.7°	NA	NA
[12]	2.28°(Mean)	5.00°	NA	99.20%
[13]	0.61°(Mean)	NA	98.69%	98.50%
MMTS – Single Mode	2.84°/3.88°(Mean)	10.94°	98.43%	99.03%
MMTS – Multi-Mode	2.88°/4.24°(Mean)	12.06°	97.83%	98.91%

comparison since the results of [12] and [13] are mean heading error. The proposed MMTS outperforms [11] significantly, while the results are better in [12] and [13]. The accurate heading in [12] and [13] is achieved by fusion of information from multiple sensors, specifically, magnetometer and gyroscope in [12], GPS and magnetometer in [13] (the tracking experiment is done outdoors). The heading performance is marginally less than [12] and [13] since the heading in MMTS is solely determined by gyroscope. The improvement with respect to [11] is achieved due to the proposed AOC scheme, compensating appropriate offset in direction for different subjects, as well as enhanced accuracy of modern sensors. The tracking result of MMTS can be viewed as raw sensor data fusion with minimum processing requirements and a promising candidate for further enhancement. Moreover, MMTS supports multiple modes of carrying the device. In [12], the mobile phone is held in hand for the entire experiment, [13] attaches the sensing device on the waist and [11] solely investigates the case when the smartphone-shaped IMU is kept in the pocket. The feature to support multiple modes is quite important since the mobile phone will not be kept in the same orientation throughout the tracking period in reality. MMTS addresses this issue and provides users of the tracking system with freedom in carrying the smartphone. This is supported by the evidence shown in Table X. The results obtained in single mode experiments are marginally better than that in multi-mode ones and they both offer satisfying and comparable tracking performance. Furthermore, MMTS delivers more reliable person-independent tracking performance assuming fewer constraints regarding the placement of the device.

Another feature of MMTS is the light-weight processing requirement, making real-time tracking feasible. It is the most computationally efficient approach compared to the referred works without using any PCA analysis [11], projection of 3-axis acceleration data from smartphone's local reference frame to a global reference frame [12] or Extended Kalman Filter [13]. The maximum processing time of individual iterations during each tracking experiment is shown in the last row of Table VIII and Table IX. Since the sensor data are sampled at 50Hz, the processing time window for one iteration is 20ms. The proposed approach implemented on the used phone achieves real-time tracking as the maximum processing time is 14.7ms. Theoretically, the iteration with maximum processing operations in MMTS is the one where a valid step is detected in HOLDING mode and calibration of the yaw data to solve 180° ambiguity is required. The reason is that HOLDING mode has extra processing to calcu-

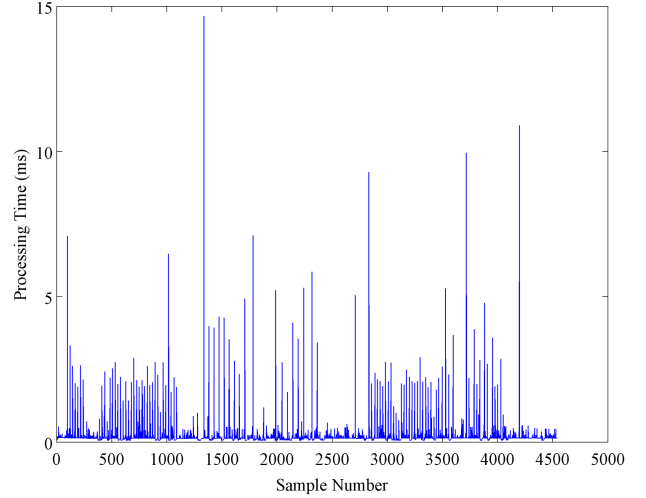


Fig. 14. Example processing time of individual iterations.

late the vertical acceleration for step detection according to equation (5) and (6) when compared to SWING and POCKET mode. This situation is covered in the path of Fig. 10(a), Fig. 13(d) and (e) as walking towards point *B* in HOLDING mode. The processing time of every iteration in the experiment corresponds to path Fig. 13(d) is also present in Fig. 14. The time also includes the time consumed in graphics updating the path on the screen. As can be seen from the figure, the maximum processing time does not appear during the last part of the experiment as analyzed theoretically above. It is observed from the processing time data for all the experiments conducted that it is unpredictable when the worst processing time appears since the phone is used normally and all the processing is scheduled by the operating system. However, the real-time processing of the MMTS is achieved as the maximum processing time is within the 20ms time window thanks to the light-weight processing characteristic of the proposed approach.

Moreover, the proposed MMTS is a scalable system not limited to indoor environment but also able to track pedestrians outdoors. The approach described in [13] achieves best heading accuracy by fusing GPS and magnetometer information but is only able to offer such accuracy outdoors. Kang and Han [12] also fuse magnetometer and gyroscope sensing, but the heading accuracy is no better than that of [13] as more unpredictable magnetic interference exists in indoor environment. MMTS is able to offer comparable tracking performance regardless of the environment as it solely dependent

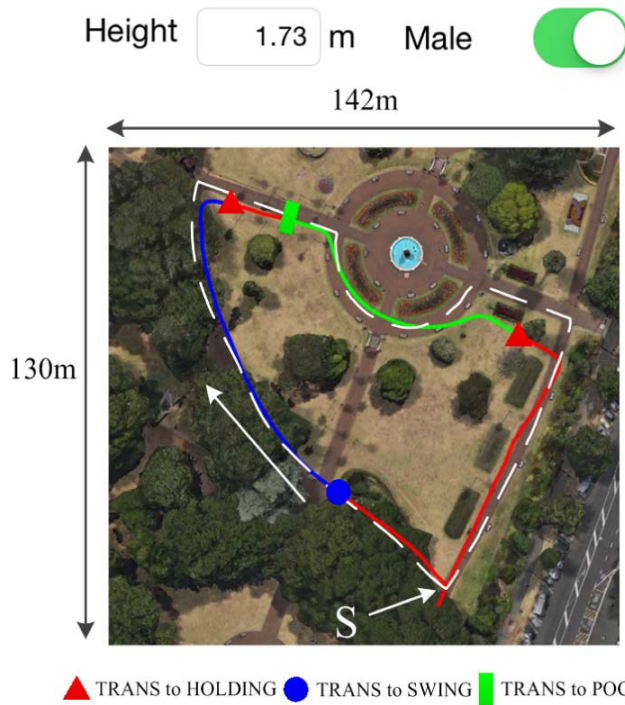


Fig. 15. Outdoor tracking path.

on the accelerometer and gyroscope within the smartphone. Typically, indoor environment is more regular with corridors, rooms separated by walls and perpendicular paths. The pedestrian is guided by the path within the closed space. While for outdoors, the path of a pedestrian will be more diverse with irregular shape in the open space. A tracking experiment under MMTS is conducted outdoors in the Albert Park, Auckland. As shown in *Fig. 15*, the white dash line outlines the shape of the path, which is irregular with curves when compared to indoors. The total length of the path is 348m. The subject starts from point S with the direction shown in the figure and returns to the same point with 458 steps. The duration of the walk is 4 minutes. The total step count and distance travelled reported by MMTS is 447 steps and 335m, with 97.6% and 96.3% accuracy respectively. An accurate tracking is also seen from the plotted track. From the result path, the maximum position error appears after the circle-shaped path in POCKET mode. It is observed that in the open space, people tend to behave differently when compared to indoors regarding the direction of walking. In the initial part of curve-shaped path in HOLDING and SWING mode, the path is guided by the edge of the lawn. While for the circle-shaped path, the references on both sides are a little further away. Under this situation, the step orientation obtained from the sensors may not reflect the walking direction of the person as sideway movements exist. Therefore, the resulting path is much smoother than the actual shape of the circle as sideway displacement is not included.

The shapes of the paths used in the experiments are further analyzed by comparing with existing works. Table XI summarizes the shapes and features of the paths used in previous works targeting pedestrian tracking. Square or rectangular

TABLE XI
SHAPE AND FEATURE OF PATHS USED IN LITERATURE

[5]	square path, 60m rectangular path, 63m J-shape path, 152m athletic track, 400m
[7]	athletic track, 400m
[12]	rectangular path with 8 turns, 168.55m
[14]	U-shape path, about 90m L-shape path, about 80m straight path, about 66m
[24]	rectangular path with 4 turns, 40m

paths are commonly seen in experimental evaluation of such systems and other irregular curved shapes such as J-shape, U-shape, L-shape and athletic track are also used. In principle, the paths contain several turns, up to 8 in [12] to verify the localization accuracy. The length of the path is typically less than 100m for indoors and can be up to 400m for outdoor application. In this paper, two paths, a 96.33m rectangular path with 4 turns and a 348m irregular curved path, are used to evaluate the proposed MMTS. The rectangular path with four turns used in indoor environment aims at testing the performance of the proposed approach on straight path with multiple turns while the irregular curved path outdoors addresses the performance of the system on curved-shaped path with continuous turns, both clockwise and anti-clockwise. These two paths were selected to demonstrate the performance of MMTS against existing approaches.

V. CONCLUSION AND FUTURE WORKS

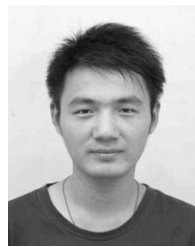
This paper proposes a smartphone-based light-weight approach, Multi-Mode PDR (MMPDR), for pedestrian tracking. The IMU in a standard smartphone is used as a walk sensor. The approach also introduces a novel step length model. It successfully identifies three typical modes of carrying the phone, calculates the step length and determines a new position in every mode. The proposed step length model is robust and accurate for people of different gender, height and walking speed. Also, an Adaptive Offset Compensation scheme introduced within the MMPDR Tracking System achieves independence on the phone carrier. The tracking performance of the proposed tracking system, developed on the commercial off-the-shelf smartphone, results in the average position accuracy of 98.91% in real-time.

Future work will be focused on extending the approach to additional modes of carrying the phone and increasing the accuracy and robustness of mode classification by fusing other observation based techniques, map and physical layout information.

REFERENCES

- [1] C.-D. Wann, Y.-J. Yeh, and C.-S. Hsueh, "Hybrid TDOA/AOA indoor positioning and tracking using extended Kalman filters," in *Proc. IEEE 63rd Veh. Technol. Conf. (VTC-Spring)*, vol. 3, May 2006, pp. 1058–1062.
- [2] L. Pei, R. Chen, J. Liu, T. Tenhunen, H. Kuusniemi, and Y. Chen, "Inquiry-based bluetooth indoor positioning via RSSI probability distributions," in *Proc. 2nd Int. Conf. Adv. Satellite Space Commun. (SPACOMM)*, Jun. 2010, pp. 151–156.

- [3] B.-G. Lee and W.-Y. Chung, "Multitarget three-dimensional indoor navigation on a PDA in a wireless sensor network," *IEEE Sensors J.*, vol. 11, no. 3, pp. 799–807, Mar. 2011.
- [4] M. N. Muhammad, Z. Salcic, and K. I.-K. Wang, "Subtractive clustering as ZUPT detector," in *Proc. IEEE 11th Int. Conf. Ubiquitous Comput.*, Bali, Indonesia, Dec. 2014, pp. 349–355.
- [5] C. Huang, Z. Liao, and L. Zhao, "Synergism of INS and PDR in self-contained pedestrian tracking with a miniature sensor module," *IEEE Sensors J.*, vol. 10, no. 8, pp. 1349–1359, Aug. 2010.
- [6] H. Fourati, "Heterogeneous data fusion algorithm for pedestrian navigation via foot-mounted inertial measurement unit and complementary filter," *IEEE Trans. Instrum. Meas.*, vol. 64, no. 1, pp. 221–229, Jan. 2015.
- [7] Z. Tian, Y. Zhang, M. Zhou, and Y. Liu, "Pedestrian dead reckoning for MARG navigation using a smartphone," *EURASIP J. Adv. Signal Process.*, vol. 2014, p. 65, Dec. 2014.
- [8] A. Mikov, A. Moschevikin, A. Fedorov, and A. Sikora, "A localization system using inertial measurement units from wireless commercial hand-held devices," in *Proc. Int. Conf. Indoor Positioning Indoor Navigat. (IPIN)*, Oct. 2013, pp. 1–7.
- [9] J. Qian, J. Ma, R. Ying, P. Liu, and L. Pei, "An improved indoor localization method using smartphone inertial sensors," in *Proc. Int. Conf. Indoor Positioning Indoor Navigat. (IPIN)*, Oct. 2013, pp. 1–7.
- [10] R. Zhang, A. Bannoura, F. Hofflinger, L. M. Reindl, and C. Schindelhauer, "Indoor localization using a smart phone," in *Proc. IEEE Sensors Appl. Symp. (SAS)*, Feb. 2013, pp. 38–42.
- [11] U. Steinhoff and B. Schiele, "Dead reckoning from the pocket—An experimental study," in *Proc. IEEE Int. Conf. Pervasive Comput. Commun. (PerCom)*, Mar./Apr. 2010, pp. 162–170.
- [12] W. Kang and Y. Han, "SmartPDR: Smartphone-based pedestrian dead reckoning for indoor localization," *IEEE Sensors J.*, vol. 15, no. 5, pp. 2906–2916, May 2015.
- [13] W. Chen, R. Chen, Y. Chen, H. Kuusniemi, and J. Wang, "An effective pedestrian dead reckoning algorithm using a unified heading error model," in *Proc. IEEE/ION Position Location Navigat. Symp. (PLANS)*, May 2010, pp. 340–347.
- [14] L.-H. Chen, E. H.-K. Wu, M.-H. Jin, and G.-H. Chen, "Intelligent fusion of Wi-Fi and inertial sensor-based positioning systems for pedestrian navigation," *IEEE Sensors J.*, vol. 14, no. 11, pp. 4034–4042, Nov. 2014.
- [15] M. G. Puyol, D. Bobkov, P. Robertson, and T. Jost, "Pedestrian simultaneous localization and mapping in multistory buildings using inertial sensors," *IEEE Trans. Intell. Transp. Syst.*, vol. 15, no. 4, pp. 1714–1727, Aug. 2014.
- [16] E. Akeila, Z. Salcic, and A. Swain, "Reducing low-cost INS error accumulation in distance estimation using self-resetting," *IEEE Trans. Instrum. Meas.*, vol. 63, no. 1, pp. 177–184, Jan. 2014.
- [17] A. R. Pratama and H. R. Widjawan, "Smartphone-based pedestrian dead reckoning as an indoor positioning system," in *Proc. Int. Conf. Syst. Eng. Technol. (ICSET)*, Sep. 2012, pp. 1–6.
- [18] J. W. Kim, H. J. Jang, D.-H. Hwang, and C. Park, "A step, stride and heading determination for the pedestrian navigation system," *J. Global Positioning Syst.*, vol. 3, nos. 1–2, pp. 273–279, 2004.
- [19] H. Weinberg, "Using the ADXL202 in pedometer and personal navigation applications," Analog Devices, Cambridge, MA, USA, Tech. Rep. AN-602, 2002.
- [20] M. Susi, V. Renaudin, and G. Lachapelle, "Motion mode recognition and step detection algorithms for mobile phone users," *Sensors*, vol. 13, no. 2, pp. 1539–1562, 2013.
- [21] H. Zhang, W. Yuan, Q. Shen, T. Li, and H. Chang, "A handheld inertial pedestrian navigation system with accurate step modes and device pose recognition," *IEEE Sensors J.*, vol. 15, no. 3, pp. 1421–1429, Mar. 2015.
- [22] J. E. A. Bertram and A. Ruina, "Multiple walking speed–frequency relations are predicted by constrained optimization," *J. Theoretical Biol.*, vol. 209, no. 4, pp. 445–453, 2001.
- [23] Q. Tian, Z. Salcic, K. I.-K. Wang, and Y. Pan, "An enhanced pedestrian dead reckoning approach for pedestrian tracking using smartphones," in *Proc. IEEE 10th Int. Conf. Intell. Sensors, Sensor Netw. Inf. Process. (ISSNIP)*, Apr. 2015, pp. 1–6.
- [24] K.-C. Lan and W.-Y. Shih, "On calibrating the sensor errors of a PDR-Based indoor localization system," *Sensors*, vol. 13, no. 4, pp. 4781–4810, 2013.
- [25] K.-C. Lan and W.-Y. Shih, "Using smart-phones and floor plans for indoor location tracking—Withdrawn," *IEEE Trans. Human-Mach. Syst.*, vol. 44, no. 2, pp. 211–221, Apr. 2014.



Qinglin Tian received the B.S. degree in electrical engineering from Zhejiang University, China, in 2011, where he is currently pursuing the Ph.D. degree with the Department of VLSI Design, College of Electrical Engineering. He was a Visiting Scholar with The University of Auckland, New Zealand, from 2014 to 2015. His research interests include design and implementation of indoor tracking and navigation systems, FPGA-based optimization and acceleration of signal processing algorithms in related area, computer architecture, and hardware-software co-design.



Zoran Salcic (SM'88) received the B.E., M.E., and Ph.D. degrees from Sarajevo University, in 1972, 1974, and 1976, respectively, all in electrical and computer engineering. He is the Chair of Computer Systems Engineering, University of Auckland. He has authored nearly 300 peer-reviewed journal and conference papers and several books. His main research interests include complex digital systems, custom-computing machines, embedded systems and their implementation, design automation tools, hardware-software co-design, models of computation and languages for concurrent and distributed systems, and cyber-physical systems. He is a Fellow of the Royal Society New Zealand and was a recipient of the Alexander von Humboldt Research Award in 2010.



Kevin I-Kai Wang received the B.E. (Hons.) degree in computer systems engineering and the Ph.D. degree in electrical and electronics engineering from the Department of Electrical and Computer Engineering, University of Auckland, New Zealand, in 2004 and 2009, respectively. He was an R&D Engineer designing home automation systems and traffic sensing systems from 2009 to 2010. From 2011 to 2013, he was with The University of Auckland as a Post-Doctoral Research Fellow and a Professional Teaching Fellow. Since 2013, he has been a Lecturer with the Department of Electrical and Computer Engineering, University of Auckland. His main research focuses on bio-cybernetic systems. His current research interests include wireless sensor network based intelligent environment, pervasive healthcare systems, industrial monitoring and automation systems, and bio-cybernetic systems.



Yun Pan received the B.S. degree from the Department of Information Science and Electronic Engineering, Zhejiang University, China, in 2002, and the Ph.D. degree from the Department of Electronic Engineering, Tsinghua University, China, in 2008. He joined the Institute of VLSI Design, College of Electrical Engineering, Zhejiang University, in 2008, as a Post-Doctoral Fellow. He is currently an Associate Professor with the College of Information Science and Electronic Engineering, Zhejiang University. His current research interests include on-chip communication, mobile computing, application-specific heterogeneous architecture design, mobile embedded systems, and healthcare micro systems. He has authored over 40 academic papers, co-authored two books and one chapter, and holds over ten Chinese patents in these areas.